Research Square

Preprints are preliminary reports that have not undergone peer review.
They should not be considered conclusive, used to inform clinical practice,
or referenced by the media as validated information.

# Multi Response Optimization of Sustainable Hybrid Aluminum Matrix Composites Reinforced NPI Slag and Eggshell for Brake Disc Applications

**Faishal Machfudz Majid**
Universitas Sebelas Maret
**Eko Surojo**
esurojo@ft.uns.ac.id
Universitas Sebelas Maret
**Dody Ariawan**
Universitas Sebelas Maret
**Wahyu Purwo Raharjo**
Universitas Sebelas Maret

**Research Article**

**Keywords:**

**Posted Date:** November 20th, 2026

**DOI:** https://doi.org/10.21203/rs.3.rs-11794969/v1

**License:** This work is licensed under a Creative Commons Attribution 4.0 International License.
Read Full License

**Additional Declarations:** No competing interests reported.

# Multi Response Optimization of Sustainable Hybrid Aluminum Matrix Composites Reinforced NPI Slag and Eggshell for Brake Disc Applications

Faishal Machfudz Majid[1,2], Eko Surojo[1*], Dody Ariawan[1], Wahyu Purwo Raharjo[1]

[1]Department of Mechanical Engineering, Universitas Sebelas Maret, Surakarta 57126, Indonesia

[2]Department of Mechanical Engineering, Faculty of Engineering, Universitas Muhammadiyah Surakarta, Sukoharjo 57162, Indonesia

*Corresponding Author: esurojo@ft.uns.ac.id

This study aims to develop environmentally friendly Hybrid Aluminum Matrix Composites (HAMC) as an alternative material for brake discs using Nickel Pig Iron (NPI) slag and eggshells (ES). The composites were fabricated by stir casting using an Al 6061 matrix, with reinforcement compositions of NPI slag, ES, graphite, and Mg designed through a Taguchi L9 orthogonal array. Microstructural, density, porosity, tensile, and Brinell hardness evaluations were conducted, followed by multi-response optimization using the Data Envelopment Analysis-based Ranking (DEAR) method. Among the nine compositions, specimen S8 (3 wt.% NPI slag, 2 wt.% ES, 1 wt.% graphite, and 1 wt.% Mg) demonstrated the best overall performance, exhibiting relatively homogeneous particle distribution, the lowest porosity (1.5%), a tensile strength of approximately 200 MPa, and an elongation of 5.8%. Although S7 achieved the highest hardness (75 BHN), its tensile strength decreased to 115 MPa, primarily due to particle agglomeration. The DEAR analysis confirmed S8 as the highest-ranked experimental composition, with an MRPI of 1.599. Mg exhibited the greatest relative influence (Delta = 1.103), and the predicted optimum factor-level combination was $NPI_2$-$ES_2$-$G_3$-$Mg_1$. These findings highlight the importance of balanced reinforcement composition, particle distribution, and porosity control in optimizing HAMC performance.

## 1. Introduction

Aluminum matrix composites (AMC) are materials that have been widely used in various applications such as automotive, maritime, aerospace, and other industries due to their higher specific strength and their ability to be tailored and designed for specific applications [1], [2]. In general, AMC is classified as an advanced material consisting of two main components: an aluminum matrix, which serves as the base material and acts as a binder, and reinforcing particles, which enhance the mechanical properties of the composite. AMC is designed to combine the desired characteristics of a metal matrix with the properties of reinforcing particles properties that are difficult to achieve with a single type of material alone [3]. Recently, the development of AMC has been limited to the use of single-reinforcement materials. As the required material specifications become more stringent, the development of AMC with dual or multiple reinforcements warrants further investigation.

Hybrid aluminum matrix composites (HAMC) are a further development of AMCs, in which the aluminum matrix is reinforced by two or more different types of reinforcement, with the aim of combining the superior properties of each type of reinforcement, thereby resulting in physical and mechanical characteristics that are superior to those of single reinforcement AMCs. [4]. Generally, the reinforcement materials used in HAMC can be divided into two broad categories based on how they are obtained. These include synthetic reinforcing materials that is, materials created through industrial manufacturing processes to replace or mimic natural materials such as $Al_2O_3$, SiC, $SiO_2$, and TiB. [5]. Another category is natural reinforcing materials, which are materials that can be obtained from nature or from waste. Some examples that can be categorized as natural materials

include waste-based materials (agricultural and industrial waste), plant-based or organic materials (rice husks, bamboo fibers), and mineral-based materials (basalt fiber, clay) [6].

One application of HAMC is in the transportation sector, where the braking system is a critical component of land vehicles for ensuring driving safety. Essentially, the braking system functions to reduce a vehicle's speed by pressing brake pads against a rotating disc to generate friction. During this process, the brake discs generate heat as a result of withstanding the friction that occurs. Therefore, further development of materials is needed to improve the performance of the braking system, particularly the brake rotor component [7]. In conventional vehicles, grey cast iron is commonly used as a material for disc rotors because it is inexpensive and readily available. However, this material has the drawbacks of being heavy, having poor wear resistance, and being susceptible to corrosion [8]. Currently, safety requirements for vehicle performance are becoming increasingly stringent. As a result, materials play a crucial role in the development of brake rotors. Given their function, brake rotors must possess high thermophysical properties, good wear resistance, superior corrosion resistance, and high stiffness [9].

This study focuses on developing HAMC using waste based reinforcing materials as an alternative material for disc rotors that supports the concept of sustainability [10]. Nickel Pig Iron (NPI) slag and eggshells (ES) were selected to improve the performance of green HAMC. It is known that Indonesia has approximately 2.6 million metric tons of nickel resources and approximately 577 million metric tons of nickel reserves. [11]. Indonesia is currently implementing a downstream industrialization program, under which raw materials are not exported; instead, products must be processed into finished or semi-finished goods. NPI is a processed product derived from laterite nickel ore, which is typically used as a raw material for stainless steel production. Industrial growth is driving an increase in NPI production. NPI production using the hot blast method generates NPI slag as a byproduct. During the production process, 1 metric ton of NPI can produce approximately 6 to 16 metric tons of slag [12]. This product cannot be reprocessed and has the potential to pollute the environment. Among the various strategies employed for waste management, applying the principles of recycling and reuse is the most appropriate approach for transforming waste into value added materials. NPI Slag has a high ceramic content, while ES is rich in organic minerals. Researchers found that NPI Slag contains 38% $SiO_2$, while ES contains 93.6% $CaCO_3$ [13], [14]. The presence of hard ceramic and mineral phases in NPI Slag and ES makes these materials potential reinforcing agents in HAMC. Compositing an aluminum matrix with ceramic particles can improve the hardness, wear resistance, and thermal conductivity of a material [15], [16]. This makes waste-based HAMC suitable for use as an alternative material for disc rotors in land vehicles.

Based on the above description, this study aims to evaluate the effect of varying the composition of NPI slag, ES, graphite, and Mg powder as reinforcing constituents on the tribomechanical characteristics of waste-based HAMC. The variations in the weight fractions of each constituent were designed using the Taguchi method to obtain the optimal composition combination. Furthermore, the DEAR (Data Envelopment Analysis-based Ranking) optimization method was applied to evaluate the multicriteria response and identify the composition combination that provides the best performance based on hardness, coefficient of friction, and wear resistance. Through this approach, this study is expected to provide insight into the contribution of each constituent and their interactions in determining the tribomechanical characteristics of HAMC based on the utilization of industrial waste and biomaterials.

## 2. Materials and Method

### 2.1 Materials

The primary materials used in the brake disc development study are aluminum, NPI slag, chicken eggshells, graphite, and magnesium (Mg) powder. Each constituent material has its own specific function, so when incorporated into HAMC, they produce a synergistic effect in accordance with the roles of the constituent materials. The classification of HAMC constituent materials is shown in Table 1.

Table 1. Classification and Functions of HAMC Constituent Materials

| Materials | Function |
|---|---|
| Al 6061 | As a matrix and binder all the constituent elements together |
| NPI Slag | Primary reinforcement, increase mechanical strength |
| Chicken egg shell | Improves physical properties, acts as a space filler, and refines the matrix grain size |
| Graphite | Solid lubricants reduce the coefficient of friction and improve tribological properties |
| Mg Powder | Reducing the surface tension and improving wettability between the matrix and the reinforcement phase |

Al 6061, with a composition of 0.85 Mg and 0.64 Si, was used as the matrix and was sourced from UD. Sutindo Sejahtera in Surabaya. As a reinforcement constituent, NPI slag was obtained from NPI processing waste at PT. Cahaya Modern Metal Industri in Cikande, Banten. The slag was processed in a ball mill and then sieved using a between140-220 mesh to obtain particles with a size of 74 μm. The composition of the NPI slag is shown in Table 2.

Table 2. Chemical Composition of NPI Slag

| Ni | $SiO_2$ | MgO | Fe | P | S | $Al_2O_3$ | CaO |
|---|---|---|---|---|---|---|---|
| 0.104 | 38.99 | 20.27 | 2.21 | 0.006 | 0.016 | 3.51 | 5.75 |

Eggshells are used as a secondary reinforcing agent in the production of HAMC. In this study, chicken eggshells obtained from food industry waste were used. The eggshells were crushed and sieved using a 300-mesh sieve to obtain particles with a size of 40 μm. To improve the tribological properties of HAMC, graphite was used as a solid lubricant. The graphite powder was obtained from Merck KGaA with a particle size of 100 mm. Fine magnesium (Mg) powder (Merck KGaA, Darmstadt, Germany) with a particle size of 0.06–0.3 mm was used to increase the surface energy of the molten metal. The presence of Mg reduces surface tension, thereby enhancing the interaction between the reinforcing agent and the molten metal and improving the wettability of the molten metal.

## 2.2 Sampel Preparation

In this study, HAMC fabrication utilized the stir casting method. The crucible containing aluminum was then placed in the electric resistance furnace of the stir casting machine and heated to 750 °C for 3 hours until complete melting was achieved. Prior to incorporation into the molten aluminum, the coated NPI slag and eggshell (ES) particles, along with graphite powder, were preheated to 500 °C to eliminate residual moisture and minimize the potential formation of porosity during composite fabrication. Once the aluminum matrix had completely melted, the reinforcing particles were gradually introduced into the melt in alternating sequences, accompanied by the addition of Mg powder according to the predetermined weight fractions. The weight fractions of the constituent

materials were designed based on the Taguchi method using an L9 orthogonal array, as shown in Table 3.

The mixing process was carried out by continuous mechanical agitation using a four-bladed impeller. The impeller was positioned at a depth equal to half the height of the molten aluminum. Agitation was maintained at a speed of 600 rpm for 10 minutes to accelerate the dispersion of the reinforcing particles throughout the liquid matrix. After the stirring process is complete, the slurry is poured into a permanent mold that has been preheated to 500°C to minimize thermal shock, and allowed to solidify for 60 minutes. After hardening, the cast specimens were removed and visually inspected to identify potential surface defects. Specimens showing no surface defects were then machined to the dimensions required for further characterization and testing.

Tabel 3. Orthogonal array

| Specimen | %Wt NPI Slag | %Wt ES | %Wt Graphite | %Wt Mg Powder |
|---|---|---|---|---|
| S1 | 1 | 1 | 0.5 | 1 |
| S2 | 1 | 2 | 1 | 1.5 |
| S3 | 1 | 3 | 1.5 | 2 |
| S4 | 2 | 1 | 1.5 | 1.5 |
| S5 | 2 | 2 | 0.5 | 2 |
| S6 | 2 | 3 | 1 | 1 |
| S7 | 3 | 1 | 1 | 2 |
| S8 | 3 | 2 | 1.5 | 1 |
| S9 | 3 | 3 | 0.5 | 1.5 |

2.3 Density and porosity

Density testing is performed to determine the mass of an object per unit volume. Corrosion testing is performed to determine the difference between the theoretical density and the actual density. The theoretical density of a sample can be determined using the rule of mixtures, as shown in Equation 1.

$$\rho_{th} = \rho_{matrix} \times V_{matrix} \times \rho_{reinforcement} \times V_{reinforcement} \quad (1)$$

Meanwhile, the actual density can be determined by applying Archimedes' principle, which can be calculated using Equation 2. During testing, the dry mass is determined by weighing the dry specimen on a scale. The wet mass is determined by placing the specimen in a measuring cylinder filled with water until it is completely submerged, and then weighing it. The porosity can then be determined once the actual and theoretical densities are known, and is calculated using Equation 3.

$$\rho_a = \frac{m_s}{m_s - m_g} \times \rho H_2O \quad (2)$$

$$\%P = 1 - \frac{\rho_a}{\rho_{th}} \times 100\% \quad (3)$$

2.4 Brinell Hardness Testing

Hardness testing was performed using the Brinell hardness method in accordance with ASTM E10-15. Before indentation, the surface of each test specimen was ensured to be smooth and flat.

Indentation was performed using a 5-mm-diameter steel ball indenter with a load of 250 kgf and a dwell time of 10 to 15 seconds. The test was conducted at three different points on each specimen. The diameter of the indentation was then measured using a microscope and calculated using Equation 4.

$$BHN = \frac{2F}{(\pi D)(D-\sqrt{D^2-d^2})} \quad (4)$$

2.5 Tensile strength

Tensile strength testing was conducted in accordance with ASTM E8 using plate-type specimens of a specific size. Tensile strength data were collected from three samples for each variation.

2.6 DEAR analysis

The DEAR method is a technique used to perform a multiresponse optimization approach that integrates several characteristics into a single composite performance value. In the DEAR method, the multiresponse performance index (MRPI) is used to evaluate several characteristics or response variables simultaneously and express them as a single quantitative value. The following are the steps involved in the DEAR method approach [17]:

1. Determining the response weights

This study evaluates the effect of the material composition of HAMC on the resulting tensile strength, hardness, and porosity values. Tensile strength (UTS) and hardness (BHN) are "larger-the-better" characteristics, which can be calculated using Equation 5, while porosity is a "smaller-the-better" characteristic that can be calculated using Equation 6.

$$W_{(UTS)i} = \frac{UTS_i}{\Sigma UTS};\ W_{(BHN)i} = \frac{BHNI_i}{\Sigma BHN} \quad (5)$$

$$W_{(porosity)i} = \frac{\left(\frac{1}{porosity_i}\right)}{\Sigma\frac{1}{porosity}} \quad (6)$$

2. Converting observed data into weighted data

After the weights are obtained, each experimental data point is multiplied by its respective response weight, as shown in Equation 7.

$$W_{ij} = Y_{ij} \times w_j \quad (7)$$

3. Determine the MRPI value by dividing the "larger-the-better" weight group by the "smaller-the-better" weight group

4. Rank based on MRPI value

## 3. Results and Discussion

3.1 Microstructure

Microstructural observations of HAMC samples with varying weight fractions of their constituents are shown in Figure 1. The microstructure reveals variations in the homogeneity and distribution of reinforcing particles resulting from differences in material composition. Specimen S8 exhibits a microstructure free of porosity, accompanied by a fine grain size. In contrast, specimens S5 and S7 exhibit a tendency toward agglomeration and more pronounced porosity, characterized by the formation of dark colored clusters with irregular morphology within the aluminum matrix. This phenomenon is believed to be related to an increase in the fraction of reinforcing particles particularly graphite and Mg which can enhance interparticle interactions through Van der Waals

forces and lead to the formation of agglomerates. The presence of agglomerates has the potential to result in non-uniform stress distribution and create local stress concentrations, thereby affecting the microstructural integrity and mechanical response of the composite.

In addition, The incorporation of ES particles may contribute to grain refinement in aluminum matrix composites through their potential influence on nucleation and grain growth behavior. Eggshells primarily consist calcium oxide (CaO) under sufficiently high-temperature conditions. Depending on their surface characteristics and crystallographic compatibility with the aluminum matrix, the resulting particles may provide additional heterogeneous nucleation sites during solidification, potentially increasing the number of nucleated aluminum grains. Furthermore, finely dispersed particles may restrict grain-boundary migration through the pinning mechanism, thereby limiting subsequent grain growth. These mechanisms could contribute to the development of a finer microstructure, provided that the reinforcement particles remain sufficiently dispersed and stable during processing.

The addition of 1 wt.% Mg to specimen S8 is believed to provide a more favorable compositional environment for the interaction between the matrix and the reinforcing particles, as reflected by a more homogeneous particle distribution and a relatively low porosity value of approximately 1.5%. This trend is consistent with the research by Hallen et al. [18], who reported that adding Mg in certain proportions can improve wetting characteristics and interfacial interactions in aluminum matrix composites. However, the effect of Mg on wetting is not always linear because it depends on temperature, atmospheric conditions, the surface characteristics of the reinforcing particles, and the potential formation of interfacial reaction products. On the other hand, increasing the Mg and graphite content in specimen S5 did not result in improved microstructural homogeneity.

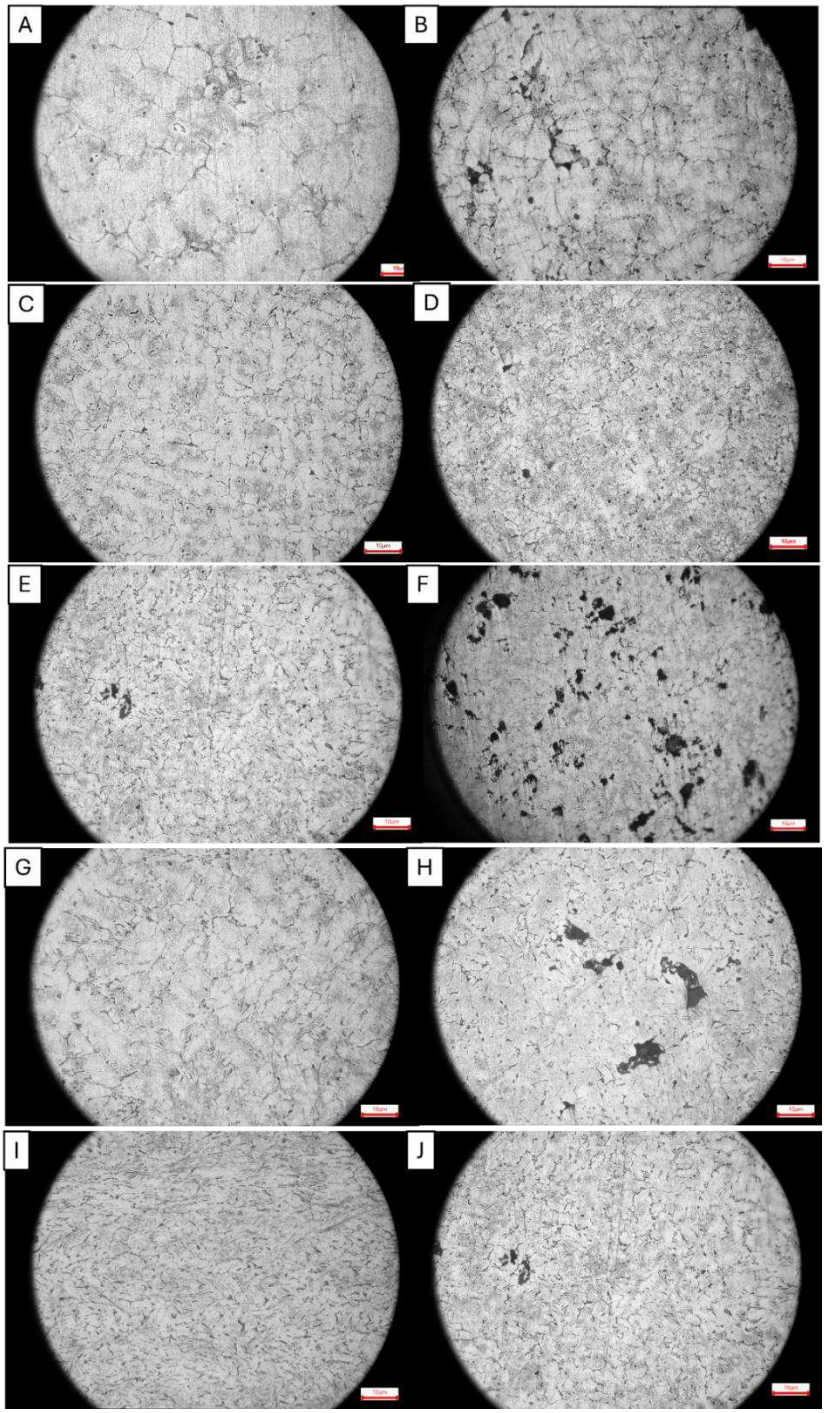



Figure 1. Microstructure HAMC Samples A) Pure Al, B) S1, C) S2, D) S3, E) S4, F) S5, G) S6, H) S7, I) S8 and J) S9

### 3.2 Density and Porosity

The physical characteristics of HAMC reveal a strong relationship between reinforcement composition, actual density, and the development of structural porosity. Compared with aluminum matrix (2.67 g/cm³), all composite specimens exhibited lower experimental density, reflecting the combined contributions of reinforcement density and processing induced defects. According to the

rule of mixtures, the theoretical density of a composite is governed by the density and volume fraction of each constituent, therefore, the incorporation of relatively low-density constituents, particularly graphite (2.1 g/cm³) and magnesium (1.73 g/cm³), may contribute to the reduction in theoretical density. Furthermore, deviations between theoretical and experimental densities indicate the presence of processing-related defects, including pores and interfacial voids. Among the investigated specimens, S5, exhibited the lowest experimental density (2.56 g/cm³) and the highest porosity (>3.3%). This behavior is consistent with its microstructural characteristics, was correlated by particle clustering. The non-uniform distribution of reinforcement particles may hinder effective matrix infiltration and promote the formation of interparticle voids. Furthermore, the relatively low density of graphite may contribute to particle segregation and clustering during mechanical stirring. Similar observations were reported by Mohanavel et al. [19] , who identified non-uniform graphite distribution in sti casting aluminum composites and attributed this behavior partly to the low density of graphite particles. In addition, excessive turbulence during stirring and subsequent metal pouring may promote air entrapment and oxide-film entrainment, which can subsequently contribute to pore formation during solidification [20] .

In contrast, specimen S8, exhibited the lowest porosity (1.5%) and a higher experimental density of (2.61 g/cm³). The relatively homogeneous reinforcement distribution observed in its microstructure suggests improved particle incorporation and reduced formation of localized voids. This favorable condition may be associated with the combined effects of reinforcement composition and the presence of Mg, which can modify the interfacial characteristics between molten aluminum and reinforcement particles, thereby promoting improved wettability and particle dispersion. Sundriyal et al. [21] demonstrated that the addition of 1 wt.% Mg to graphite-reinforced aluminum composites improved particle distribution and composite properties through enhanced wetting conditions. Similarly, Malaki et al. [22] highlighted the important role of Mg in modifying interfacial energy and improving reinforcement wettability in aluminum-based metal matrix composites. Nevertheless, the lower porosity of S8 should not be attributed exclusively to Mg addition, since reinforcement fraction, particle characteristics, stirring conditions, and melt quality also influence porosity development. In particular, excessive stirring may promote oxide film entrainment, while inadequate degassing can allow dissolved hydrogen to contribute to pore formation during solidification. These mechanisms are well established in aluminum casting systems [23], [24]. Consequently, the comparison between S5 and S8 indicates that the physical integrity of HAMCs is governed not simply by the total reinforcement content, but by the balance between constituent density, particle dispersion, interfacial wettability, and casting conditions. The lower porosity and higher experimental density obtained in S8 therefore indicate a more favorable combination of composition and processing conditions among the investigated specimens.

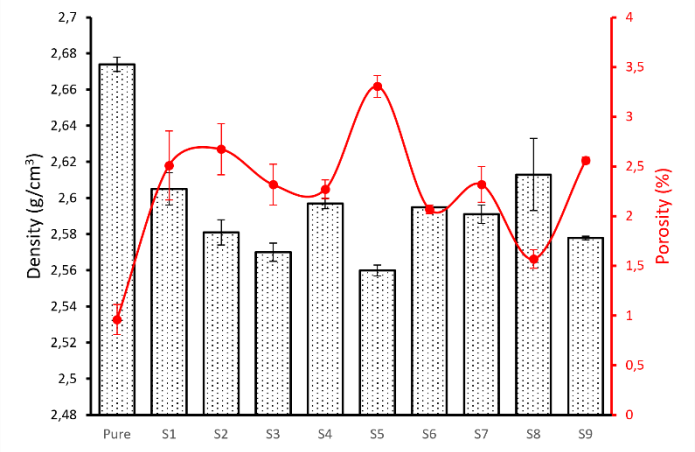



Figure 2. Actual density and %porosity of HAMC samples

### 3.3 Tensile Strength

The tensile properties of HAMC exhibited a strong dependence on reinforcement composition and microstructural integrity. Compared with the unreinforced aluminum matrix, which exhibited a UTS of ~120 MPa, specimens S5 and S8 showed improved tensile strengths of 145 and 200 MPa, respectively, whereas S7 exhibited lowest UTS of ~115 MPa, indicating no substantial improvement over the matrix. The highest tensile performance was achieved by S8, which combined a UTS of 200 MPa with an elongation of 5.8%. This simultaneous improvement in strength and ductility suggests more effective stress transfer from the ductile aluminum matrix to the dispersed reinforcement particles, particularly the mineral rich NPI slag and eggshell derived particles. The fine microstructure observed in S8, together with its relatively high actual density (2.61 g/cm³) and lowest porosity (1.5%), supports this interpretation by indicating fewer microstructural defects that could initiate premature fracture. The addition of 1 wt.% Mg may also have contributed to improved particle wettability and dispersion during stir casting.

In contrast, S7 exhibited a pronounced reduction in tensile performance, with a UTS of ~115 MPa and an elongation of 1.5%, despite recording the highest Brinell hardness (75 BHN). The relatively high graphite and Mg contents in this specimen may have further affected particle distribution and interfacial conditions; nevertheless, their individual contributions cannot be isolated from the present results. A similar, although less pronounced, reduction in mechanical performance was observed in S5, which exhibited a UTS of 145 MPa and an elongation of 2.8%. Its lowest experimental density (2.56 g/cm³), highest porosity (>3.3%), and non-uniform particle distribution indicate a greater population of potential defects that can reduce the effective load bearing area and promote local stress concentration, void growth, and subsequent void coalescence during tensile deformation. These observations are consistent with Suthar et al. [25] , who demonstrated that reinforcement clustering and porosity significantly affect the UTS of stir-cast hybrid aluminum composites, and this finding was support by Grilo et al. [26] , who emphasized the importance of particle wettability, dispersion, and de-agglomeration in determining the mechanical performance of casting-based aluminum composites.

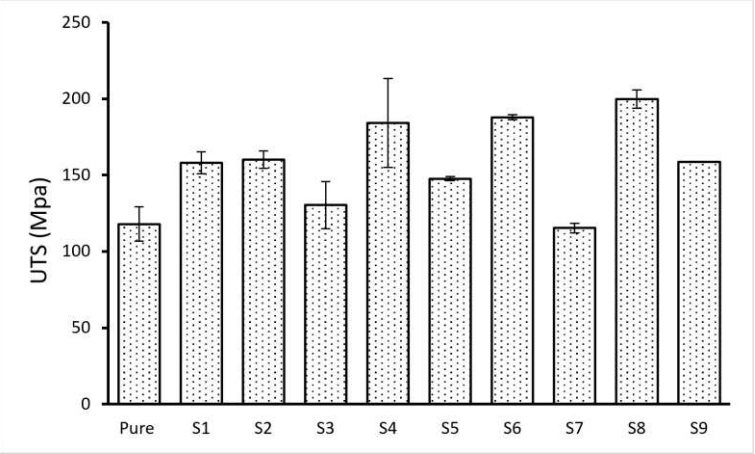



Figure 3. Tensile strength of HAMC samples

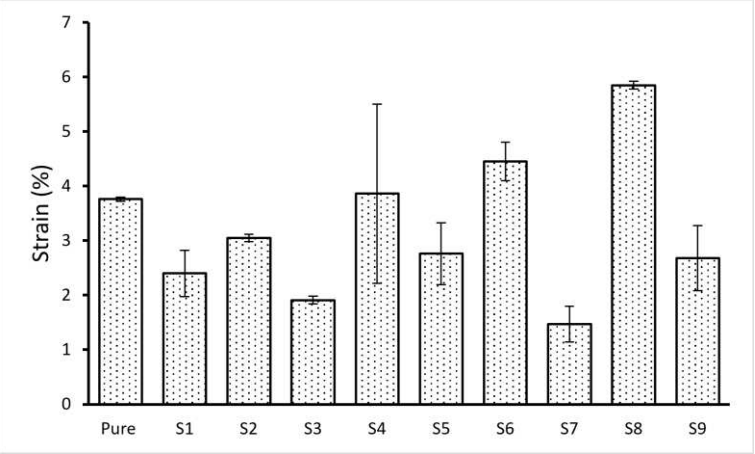



Figure 4. Yield strength of HAMC samples

### 3.4 Brinell Hardness

The Brinell hardness test revealed that all HAMC specimens exhibited higher hardness than the unreinforced aluminum matrix (47 BHN). The hardness increased to 72 BHN for S5, 75 BHN for S7, and 63 BHN for S8, corresponding to improvements of approximately 53.2%, 59.6%, and 34.0%, respectively. This enhancement can primarily be attributed to the incorporation of NPI slag and ES particles, which may restrict localized plastic deformation and impede dislocation movement within the aluminum matrix. The contribution of graphite and Mg powder should also be considered in relation to their respective functions: graphite is a relatively soft solid lubricant, whereas Mg primarily acts as a wetting promoting additive in the molten aluminum system and may contribute to solid solution strengthening if dissolved in the matrix. Consequently, the relationship between reinforcement fraction and hardness is not necessarily linear because it depends on the type, proportion, particle characteristics, interfacial bonding, and distribution of each constituent. In addition to dispersion strengthening, particle incorporation may contribute to grain refinement by promoting heterogeneous nucleation during solidification or restricting grain boundary migration through particle pinning. These mechanisms can increase the resistance to dislocation motion, consistent with the Hall Petch relationship, in which strength increases as the average grain size decreases [27] .

Despite the overall hardness enhancement, the differences among the specimens indicate that reinforcement distribution and casting defects strongly influence the measured hardness. S7 exhibited the highest hardness (75 BHN), but its microstructure showed severe particle agglomeration, accompanied by a relatively low ultimate tensile strength (UTS) of approximately 115 MPa. The locally concentrated reinforcement-rich regions may have increased the resistance to Brinell indentation at particular measurement locations; however, such localized resistance does not necessarily represent uniform strengthening of the entire composite. A similar interpretation applies to S5, which exhibited a hardness of 72 BHN despite having the lowest actual density (2.56 g/cm³) and the highest porosity (>3.3%). The combination of particle clustering and pores can generate microstructural heterogeneity, reduce the effective load bearing area, and create stress concentration sites that impair the overall mechanical integrity. In contrast, S8 exhibited a more balanced mechanical response, with a hardness of 63 BHN, an acrual density of 2.61 g/cm³, the lowest porosity (1.5%), and the highest UTS (200 MPa). Its relatively homogeneous particle distribution suggests that the reinforcement particles were incorporated more effectively into the aluminum matrix, allowing a more consistent contribution to local deformation resistance while minimizing defects associated with agglomeration and porosity. These observations agree with previous studies reporting that reinforcement fraction, particle wettability, and dispersion quality jointly determine the hardness and mechanical performance of stir-cast aluminum composites [28]. Therefore, the results indicate that the highest hardness does not necessarily correspond to the best overall mechanical performance; rather, a combination of adequate reinforcement content, homogeneous particle distribution, and low porosity is essential for achieving a more balanced hardness strength response.

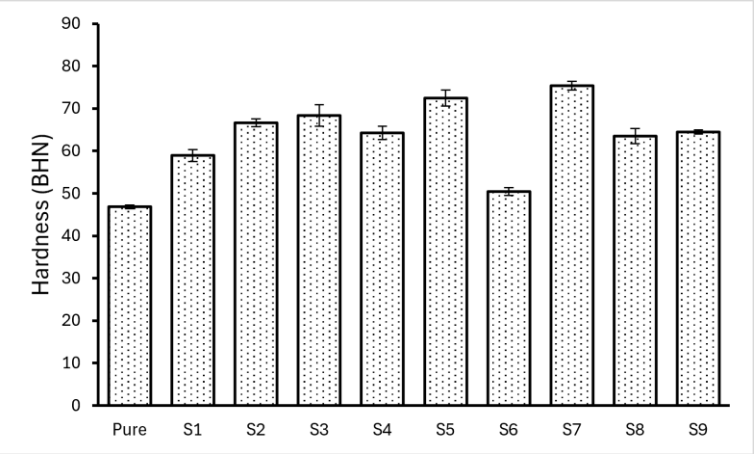



Figure 5. HAMC Brinell hardness value

3.5 DEAR analysis

Table 4. Weight responses of Hardness (BHN), tensile strength (UTS) an %porosity of HAMC characteristics

| Sample | BHN | $W_{BHN}$ | UTS | $W_{UTS}$ | %Porosity | $W_{\%Porosity}$ |
|---|---|---|---|---|---|---|
| S1 | 58.910 | 0,101 | 158,04 | 0,109606142 | 2,51 | 8,603187251 |
| S2 | 66.638 | 0,114 | 160,11 | 0,111041758 | 2,673 | 8,078563412 |

| | | | | | | |
|---|---|---|---|---|---|---|
| S3 | 68.352 | 0,117 | 130,29 | 0,090360568 | 2,317 | 9,319810099 |
| S4 | 64.299 | 0,110 | 184,2 | 0,127748996 | 2,271 | 9,508586526 |
| S5 | 72.473 | 0,124 | 147,64 | 0,102393386 | 3,306 | 6,531760436 |
| S6 | 50.468 | 0,086 | 187,83 | 0,130266525 | 2,069 | 10,43692605 |
| S7 | 75.378 | 0,129 | 115,33 | 0,079985297 | 2,319 | 9,311772316 |
| S8 | 63.479 | 0,109 | 199,69 | 0,138491841 | 1,569 | 13,76290631 |
| S9 | 64.492 | 0,110 | 158,76 | 0,110105487 | 2,56 | 8,43515625 |

Table 5. Weight response data and MRPI values

| Sample | P $(BHN \times W_{BHN})$ | Q $(UTS \times W_{UTS})$ | R $(\%Porosity \times W_{\%Porosity})$ | MRPI $(P + Q/R)$ | Rank |
|---|---|---|---|---|---|
| S1 | 5,937 | 17,32215467 | 21,594 | 1,077131475 | 7 |
| S2 | 7,598 | 17,77889582 | 21,594 | 1,175161638 | 4 |
| S3 | 7,993 | 11,77307846 | 21,594 | 0,915366242 | 8 |
| S4 | 7,073 | 23,53136508 | 21,594 | 1,417284193 | 2 |
| S5 | 8,986 | 15,11735958 | 21,594 | 1,116213507 | 6 |
| S6 | 4,358 | 24,46796143 | 21,594 | 1,334892279 | 3 |
| S7 | 9,721 | 9,224704312 | 21,594 | 0,87736146 | 9 |
| S8 | 6,894 | 27,65543564 | 21,594 | 1,599963328 | 1 |
| S9 | 7,116 | 17,48034704 | 21,594 | 1,139031648 | 5 |

Table 6. MRPI value for each level of the research factor

| Factors | Levels | | | Max-Min (Δ) |
|---|---|---|---|---|
| | 1 | 2 | 3 | |
| Wt% NPI Slag | 3,167659356 | **3,868389979** | 3,616356435 | 0,700730623 |
| Wt% ES | 3,371777128 | **3,891338473** | 3,389290169 | 0,519561345 |
| Wt% Graphite | 3,332376631 | 3,387415377 | **3,932613763** | 0,600237132 |
| Wt% Mg Powder | **4,011987082** | 3,731477479 | 2,908941209 | 1,103045873 |

Bold writing indicates these level have the most impact on HAMC performance

The multi-response optimization results presented in Table 5 indicate that specimen S8 achieved the highest Multi-Response Performance Index (MRPI) of 1.599, ranking first among all investigated specimens, whereas S7 exhibited the lowest MRPI of 0.877 (rank 9). The superior overall performance of S8 was primarily associated with its high ultimate tensile strength (UTS) of 199.69 MPa and relatively low porosity of 1.569%, demonstrating the importance of maintaining an appropriate balance between mechanical strength and casting quality. In contrast, although S7

exhibited the highest Brinell hardness (75.378 BHN), its substantially lower UTS (115.33 MPa) and higher porosity resulted in the lowest overall performance. This behavior suggests that excessive reinforcement agglomeration and non-uniform particle distribution may generate stress concentration sites and weaken interfacial load transfer, consequently promoting crack initiation under tensile loading. These findings indicate that hardness enhancement alone does not necessarily translate into improved tensile performance, particularly when accompanied by increased porosity. Furthermore, the relationship between density and porosity provides additional evidence for evaluating composite integrity, as lower porosity generally contributes to higher relative density and improved resistance to tensile failure. Therefore, the superior MRPI of S8 reflects a more favorable combination of hardness, tensile strength, and porosity compared with the other investigated compositions.

As presented in Table 6, Mg addition exhibited the highest Delta (Max–Min) value of 1.103, followed by NPI slag (0.700), graphite (0.600), and eggshell (ES) (0.519), indicating that Mg was the most influential factor affecting the overall performance of HAMC within the investigated composition range. This behavior can be associated with the role of Mg as a wetting promoting alloying addition, which can improve the interaction between molten aluminum and reinforcement particles, facilitate particle incorporation, and potentially reduce particle agglomeration and interfacial defects during stir casting. Furthermore, Table 6 identifies the optimum factor levels as NPI slag level 2 (MRPI = 3.868), ES level 2 (3.891), graphite level 3 (3.932), and Mg level 1 (4.011), corresponding to the predicted optimum combination. The selection of the lowest Mg level suggests that a moderate Mg addition is more favorable than excessive addition under the investigated processing conditions. Meanwhile, the incorporation of hard NPI slag and ES particles may contribute to localized deformation resistance, while graphite can influence the friction and wear behavior of the composite. Nevertheless, the effectiveness of these hybrid reinforcements depends on their distribution, interfacial bonding, and the resulting porosity level. Consequently, the optimum composition should be considered in conjunction with the density, porosity, hardness, and tensile results to establish the overall relationship between reinforcement characteristics, composite densification, and mechanical performance.

## 4. Conclusion

The results demonstrate that the hybrid reinforcement composition strongly influences the microstructure and mechanical performance of HAMC. Among the tested specimens, S8 (3 wt.% NPI slag, 2 wt.% ES, 1 wt.% graphite, and 1 wt.% Mg) exhibited the best overall performance, with a relatively homogeneous particle distribution, the highest experimental density (2.61 g/cm$^3$), the lowest porosity (1.569%), a UTS of 199.69 MPa, an elongation of 5.8%, and a hardness of 63 BHN. In contrast, particle agglomeration in S5 and S7 deteriorated the composite integrity, as reflected by the low tensile performance of S7 (UTS of 115.33 MPa and elongation of 1.5%), despite its highest hardness (75.378 BHN). The DEAR analysis further confirmed S8 as the best-performing experimental composition, with the highest MRPI of 1.599, while Mg showed the greatest relative influence ($\Delta$ = 1.103), followed by NPI slag, graphite, and ES. The predicted optimum factor-level combination was $NPI_2$-$ES_2$-$G_3$-$Mg_1$. Overall, these findings establish that balanced reinforcement composition, uniform particle distribution, and porosity control are essential to achieving an optimal combination of strength, hardness, and ductility in HAMC.

## 5. Acknowledgement

The authors sincerely acknowledge invaluable support and research facilities of Universitas Sebelas Maret (UNS) under scheme of "*PENELITIANs PASCASARJANA DOKTOR (PPs DOKTOR UNS) Batch 2*" with contract number 973.1/UN27.22/PT.01.03/2026.

## 6. References

[1] N. Idusuyi and J. I. Olayinka, "Dry sliding wear characteristics of aluminium metal matrix composites: a brief overview," *Journal of Materials Research and Technology*, vol. 8, no. 3, pp. 3338–3346, May 2019, doi: 10.1016/j.jmrt.2019.04.017.

[2] A. Mussatto, I. U. Ahad, R. T. Mousavian, Y. Delaure, and D. Brabazon, "Advanced production routes for metal matrix composites," *Engineering Reports*, vol. 3, no. 5, May 2021, doi: 10.1002/eng2.12330.

[3] S. Mohan Kumar, R. Pramod, and H. K. Govindaraju, "Evaluation of Mechanical and Wear Properties of Aluminium AA430 Reinforced with SiC and Mgo," *Mater. Today Proc.*, vol. 4, no. 2, pp. 509–518, 2017, doi: 10.1016/j.matpr.2017.01.051.

[4] N. Ashrafi, A. H. M. Ariff, M. Sarraf, S. Sulaiman, and T. S. Hong, "Microstructural, thermal, electrical, and magnetic properties of optimized Fe3O4–SiC hybrid nano filler reinforced aluminium matrix composite," *Mater. Chem. Phys.*, vol. 258, p. 123895, Jan. 2021, doi: 10.1016/j.matchemphys.2020.123895.

[5] M. O. Bodunrin, K. K. Alaneme, and L. H. Chown, "Aluminium matrix hybrid composites: a review of reinforcement philosophies; mechanical, corrosion and tribological characteristics," *Journal of Materials Research and Technology*, vol. 4, no. 4, pp. 434–445, Oct. 2015, doi: 10.1016/j.jmrt.2015.05.003.

[6] H. I. Akbar, E. Surojo, and D. Ariawan, "Investigation of Industrial and Agro Wastes for Aluminum Matrix Composite Reinforcement," *Procedia Structural Integrity*, vol. 27, pp. 30–37, 2020, doi: 10.1016/j.prostr.2020.07.005.

[7] K. Reif, Ed., *Brakes, Brake Control and Driver Assistance Systems*. Wiesbaden: Springer Fachmedien Wiesbaden, 2014. doi: 10.1007/978-3-658-03978-3.

[8] S. A. Awe, "Developing Material Requirements for Automotive Brake Disc," *Modern Concepts in Material Science*, vol. 2, no. 2, Nov. 2019, doi: 10.33552/MCMS.2019.02.000531.

[9] A. Rashid, "Overview of disc brakes and related phenomena - a review," *International Journal of Vehicle Noise and Vibration*, vol. 10, no. 4, p. 257, 2014, doi: 10.1504/IJVNV.2014.065634.

[10] B. Prabhu *et al.*, "Cleaner production of performance-enhanced hybrid composites using agro-industrial wastes: A sustainable waste management strategy," *J. Environ. Manage.*, vol. 381, p. 125116, May 2025, doi: 10.1016/j.jenvman.2025.125116.

[11] R. Andika, W. Astuti, Syafriadi, and F. Nurjaman, "Effect of flux addition and reductant type in smelting process of Indonesian limonite ore in electric arc furnace," *IOP Conf. Ser. Mater. Sci. Eng.*, vol. 478, p. 012007, Feb. 2019, doi: 10.1088/1757-899X/478/1/012007.

[12] A. T. M. Marsh, T. Yang, S. Adu-Amankwah, and S. A. Bernal, "Utilization of metallurgical wastes as raw materials for manufacturing alkali-activated cements," in *Waste and Byproducts in Cement-Based Materials*, Elsevier, 2021, pp. 335–383. doi: 10.1016/B978-0-12-820549-5.00009-7.

[13] J. Neunzehn, T. Szuwart, and H.-P. Wiesmann, "Eggshells as natural calcium carbonate source in combination with hyaluronan as beneficial additives for bone graft materials, an in vitro study," *Head Face Med.*, vol. 11, no. 1, p. 12, Dec. 2015, doi: 10.1186/s13005-015-0070-0.

[14] A. Setyani, Y. Amalia, and H. R. Wardhana, "Potensi dan Karakterisasi Limbah Metalurgi 'Slag Nikel Pig Iron,'" *Journal of Metallurgical Engineering and Processing Technology*, vol. 3, no. 2, p. 132, Feb. 2023, doi: 10.31315/jmept.v3i2.8579.

[15] I. K. G. Sugita, K. Suarsna, N. P. G. Suardana, and R. Sunoko, "Improvement of wear-resistant and thermal conductivity of aluminum matrix composite reinforced AL2O3/SiCw/Mg powder," *Eastern-European Journal of Enterprise Technologies*, vol. 4, no. 12 (130), pp. 6–14, Aug. 2024, doi: 10.15587/1729-4061.2024.308704.

[16] R. AM, M. Kaleemulla, S. Doddamani, and B. KN, "Material characterization of SiC and Al2O3–reinforced hybrid aluminum metal matrix composites on wear behavior," *Advanced Composites Letters*, vol. 28, 2019, doi: 10.1177/0963693519856356.

[17] K. . Krishnaian and P. . Shahabudeen, *Applied design of experiments and taguchi methods*. PHI Learning Private Limited, 2012.

[18] J. M. Hallen, H. M. Balmori, D. Jaramillo-Vigueras, J. L. Estrada, J. L. González, and A. Manzano-Ramírez, "Influence of Mg and Stirring on the Strength of an Aluminium Matrix Composite Obtained by Compocasting," *Key Eng. Mater.*, vol. 127–131, pp. 495–502, Nov. 1996, doi: 10.4028/www.scientific.net/KEM.127-131.495.

[19] V. Mohanavel, K. Rajan, S. Suresh Kumar, G. Vijayan, and M. S. Vijayanand, "Study on mechanical properties of graphite particulates reinforced aluminium matrix composite fabricated by stir casting technique," *Mater. Today Proc.*, vol. 5, no. 1, pp. 2945–2950, 2018, doi: 10.1016/j.matpr.2018.01.090.

[20] M. A. El-Sayed, H. Hassanin, and K. Essa, "Bifilm defects and porosity in Al cast alloys," *The International Journal of Advanced Manufacturing Technology*, vol. 86, no. 5–8, pp. 1173–1179, Sep. 2016, doi: 10.1007/s00170-015-8240-6.

[21] P. Sundriyal and P. L. Sah, "Enhancement of Mechanical Properties of Graphite Particulate Aluminum Metal Matrix Composites by Magnesium Addition," *Mater. Today Proc.*, vol. 4, no. 9, pp. 9481–9486, 2017, doi: 10.1016/j.matpr.2017.06.208.

[22] M. Malaki, A. Fadaei Tehrani, B. Niroumand, and M. Gupta, "Wettability in Metal Matrix Composites," *Metals (Basel).*, vol. 11, no. 7, p. 1034, Jun. 2021, doi: 10.3390/met11071034.

[23] J. Grilo, V. H. Carneiro, J. C. Teixeira, and H. Puga, "Manufacturing Methodology on Casting-Based Aluminium Matrix Composites: Systematic Review," *Metals (Basel).*, vol. 11, no. 3, p. 436, Mar. 2021, doi: 10.3390/met11030436.

[24] M. A. El-Sayed, H. Hassanin, and K. Essa, "Bifilm defects and porosity in Al cast alloys," *The International Journal of Advanced Manufacturing Technology*, vol. 86, no. 5–8, pp. 1173–1179, Sep. 2016, doi: 10.1007/s00170-015-8240-6.

[25] J. Suthar and K. Patel, "Identification, screening and optimization of significant parameters for stir cast hybrid aluminium metal matrix composite," *Heliyon*, vol. 4, no. 12, p. e00988, Dec. 2018, doi: 10.1016/j.heliyon.2018.e00988.

[26] J. Grilo, V. H. Carneiro, J. C. Teixeira, and H. Puga, "Manufacturing Methodology on Casting-Based Aluminium Matrix Composites: Systematic Review," *Metals (Basel).*, vol. 11, no. 3, p. 436, Mar. 2021, doi: 10.3390/met11030436.

[27] J. Nie *et al.*, "Key roles of particles in grain refinement and material strengthening for an aluminum matrix composite," *Materials Science and Engineering: A*, vol. 801, p. 140414, Jan. 2021, doi: 10.1016/j.msea.2020.140414.

[28] S. C. Udensi and A. U. Anioke, "An in-depth investigation of factors responsible for optimal performance in stir-cast Aluminum metal matrix composites," *Sci. Afr.*, vol. 26, p. e02452, Dec. 2024, doi: 10.1016/j.sciaf.2024.e02452.